RSC Advances

PAPER

View Article Online
View Journal | View Issue



Cite this: *RSC Adv.*, 2015, **5**, 19166

# Characterization, performance, and applications of a yeast surface display-based biocatalyst†

J. M. Eby and S. W. Peretti*

Received 12th December 2014
Accepted 6th February 2015

DOI: 10.1039/c4ra16304d

www.rsc.org/advances

This work demonstrates the efficacy and cost effectiveness of yeast surface display (YSD) as a method for producing and purifying enzyme catalysts. Lipase B from *Candida antarctica* (CalB) and lipase from *Photobacterium lipolyticum* sp. M37 (M37L) were individually displayed on the surface of yeasts *via* fusion with alpha-agglutinin. The enzyme is produced, purified, and immobilized in a single step. The population expressing the enzyme was quantified by flow cytometry. After lyophilization, the hydrolytic activity of the biocatalyst was assayed with *p*-nitrophenyl butyrate and *p*-nitrophenyl palmitate substrates. Esterification reactions involving octanoic acid and either butanol or octanol were used to evaluate esterification activity. The lyophilized YSD biocatalyst hydrolytic activity matched or exceeded commercial lipase (Novozym 435) immobilized on acrylic resin at equal catalyst loading, and achieved esterification levels 10–50% that of Novozyme 435. Factoring in the cost of production, the YSD biocatalyst represents a considerable savings over traditionally prepared and purchased enzyme catalysts. This promises to significantly expand the catalytic applications of immobilized lipases, and immobilized enzymes more generally, in commercial processes.



## Introduction

The cost of purified enzyme is a primary obstacle to its commercial implementation. Despite the variety of ways that enzymes can be prepared for industrial use,[1] up to 80% of the final cost is associated with purification and immobilization.[2,3] Display of the enzyme on the surface of the production organism offers the potential for dramatic decreases in cost and catalyst preparation time. While yeast surface display (YSD) was developed to succeed phage and bacterial display as a tool for protein engineering,[4] parallel applications in biocatalysis were quickly identified.[5] Enzymes displayed on the yeast cell surface take advantage of the yeasts' production efficiency and selective protein display. Using the yeast as the production host *and* as the final catalytic support circumvents the most costly steps in enzyme preparation. An additional benefit comes from the fungal cell wall, a rigid structure composed of glucans, mannoproteins, and chitin,[6] which offers physically and chemically robust support. The two most prevalent and flexible methods for displaying proteins on the yeast surface employ either an α-agglutinin fusion (covalent cell wall attachment[4]) or fusion to a truncated yeast flocculin protein (non-covalent adhesion[7]). Proteins ranging in size from a DNA binding motif (7 kDa)[8] to β-glucosidase (136 kDa)[9] have been displayed on the yeast surface and retained their function, demonstrating the capacity and flexibility of the system.

Lipases are of particular utility in surface display systems for several reasons: they catalyze many synthetic reactions; they are relatively thermostable and promiscuous; they require no cofactors or regeneration; they are stable and active in some organic solvents; and they are active extracellularly without modification.[10,11] Lipase B from *Candida antarctica* (CalB) is a widely-studied industrial enzyme whose crystal structure has been solved,[12] but whose application to esterification is somewhat limited by its susceptibility to methanol deactivation.[13] Recently, a lipase, M37L, from a psychrophilic bacterium (*P. lipolyticum* sp. M37) with better tolerance of high methanol concentrations,[14] has been applied to a biodiesel reaction.[15] Most recently, directed evolution was used to dramatically enhance methanol tolerance and thermal stability for a lipase from *Proteus mirabilis*.[16]

Investigators have had success immobilizing lipases using surface display in bacteria,[17] filamentous fungi,[18] and yeast.[19–21] Bielen *et al.* published a systematic review of surface display as it applies to lipolytic enzymes.[22] The use of yeast, especially *Saccharomyces* sp., is appealing because of the genus' rapid growth, mapped genome and proteome, and facile genetic manipulation. Many fungal lipases have been displayed on yeast, including lipases from *Rhizomucor miehei*,[23] *Rhizopus oryzae*,[20,24] and *Candida antarctica*.[25,26]

The activity of surface-displayed M37L is reported here for the first time. The previous attempt at immobilization used enzyme cross-linking, and the aggregate produced methyl

*North Carolina State University, Department of Chemical and Biomolecular Engineering, 911 Partners Way, Raleigh, NC 27695-7905, USA. E-mail: peretti@ncsu.edu*

† Electronic supplementary information (ESI) available. See DOI: 10.1039/c4ra16304d

esters from olive oil at 70% conversion.[27] Since immobilization can often result in an increase in stability and activity,[19] M37L and wild-type CalB have been incorporated into a YSD fusion for comparison.

Activity is reported here in terms of conversion, normalized by catalyst dry mass. Activity for YSD-based biocatalysts is typically reported as a bulk property, in arbitrary units that neglect catalyst loading, making replication of the results difficult. These characterizations ignore the dynamics of the production organism and rely on commonly cited assumptions about the amount of catalytic protein being produced.[19,28] Here, analysis of the population by flow cytometry has been applied to optimize the production of the biocatalyst towards uniformly high surface display of the lipase.

## Results

### Flow cytometry

Cells are selected for analysis according to their forward scatter and side scatter distributions (roughly correlated to size and granularity, respectively). In a linear side scatter *vs.* forward scatter (SS *vs.* FS) plot, ≥80% of the total population is typically gated for analysis (P2 in Fig. 1). The gated population in P2 decreases approximately 10% after lyophilization, indicating a partial loss of cell integrity during the process. After lyophilization, a new

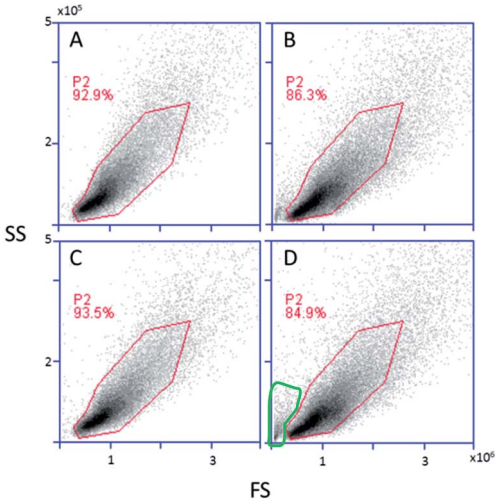


Fig. 1 SS *vs.* FS plots for the ycM37L yeast biocatalyst. Intact cells are gated based on their characteristic size and granularity (P2), based on the unlabeled sample (A), and the gate is applied to the histograms in Fig. 2–4. Small changes in the population's physical characteristics upon lyophilization (B) are discussed in the text. Immuno-labeling of the surface construct had no significant effect on either the live (C) or the lyophilized cells (D).

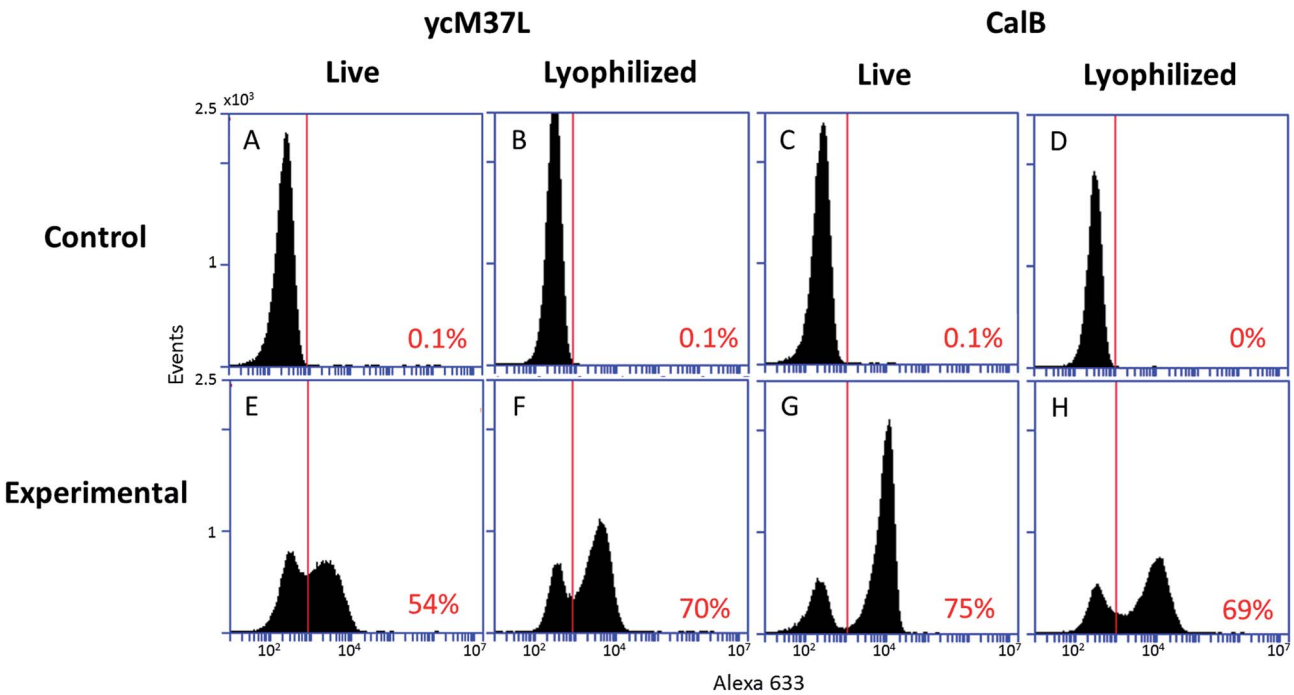


Fig. 2 Representative histograms for the yeast biocatalysts, with the percentage of the population above the vertical gate at bottom right. The population gated in Fig. 1 is labeled with antibodies specific to the C-terminal epitope in the surface construct. From histograms of fluorescence intensity, the background is determined by setting a gate such that less than 1% of an unlabeled control lies to the right. The population with higher fluorescence (to the right of the gate) than the control is expressing the SD construct, including the lipase. The population with higher fluorescence than the control (to the right of the gate) is expressing the SD construct, including the lipase. Background from labeling with only the secondary antibody is low (A–D). The majority of the population is expressing the surface construct before and after lyophilization (E–H). The histograms shown are from four independent cultures and cytometry experiments. A reduction in the fraction expressing the construct is observed if culture conditions are sub-optimal (E, shown for demonstration).

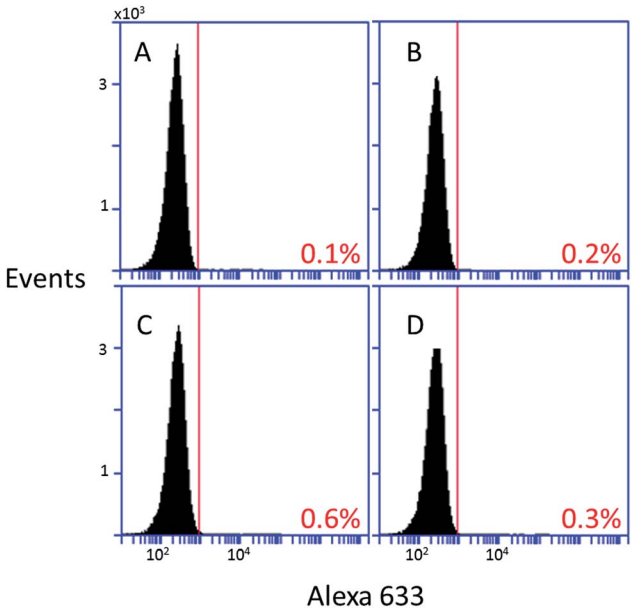


Fig. 3 Histograms for the YSD CalB biocatalyst expressed in a high-copy vectors. The fraction of the population expressing the construct after one round (C) or two rounds of sorting (D) is not appreciably higher than untransformed MT8-1 cells (A) or cells labeled without the primary antibody (B). The same trend is observed in cells displaying ycM37L.

population appears in the lower left of the SS *vs.* FS plots, indicating an increase in cell debris (highlighted by a green polygon, Fig. 1D). The lyophilized cells are permeable to propidium iodide, which further supports the theory that losses are due to physical degradation. For single-copy plasmids (pCT-CalB and pCT-ycM37L), the construct is detected in >69% of the gated population under the culture and lyophilization conditions described below (Fig. 2F and H). After lyophilization, the expressing population is typically ≥90% of that before lyophilization. Storage of the cells in buffer or in culture medium at 4 °C for more than 24 hours also results in a loss of the surface construct, which suggests that lyophilization is preferable for long-term storage.

Codon optimization of M37L increased the population expressing detectable protein on the surface from <1% (ESI†) to the same range as that of CalB (Fig. 2). However, the average fluorescent intensity in the ycM37L-expressing population is routinely 2- to 4-fold lower than that of the CalB-expressing population.

For the high-copy plasmid, no greater than 1% of the population was observed to express the SD fusion (Flo1S-lipase-c-myc) after two rounds of cell sorting (Fig. 3). The plasmid and insert were present and the DNA sequence was confirmed. The likely cause of failure to detect the construct is over-saturation of the cellular translation and secretion machinery. Because little-to-no fusion protein was detected on the cell surface, the high-copy cells were not tested for lipase activity.

Table 1 Observed copy number of lipase on YSD biocatalyst. Values were determined by interpolating a standard curve, and are the average of five samples prepared in parallel

| Enzyme displayed | Average copy number | Standard deviation ($N = 5$) |
|---|---|---|
| CalB | 48 423 | 5983 |
| ycM37L | 22 739 | 1314 |

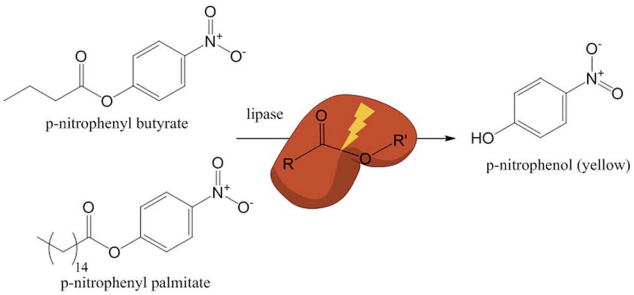


Scheme 1

## Copy number

The measured copy numbers on lyophilized CalB- and ycM37L-displaying yeast cells are given in Table 1. Approximately 48 000 and 23 000 copies of the SD construct were observed on the CalB and ycM37L biocatalysts, respectively.

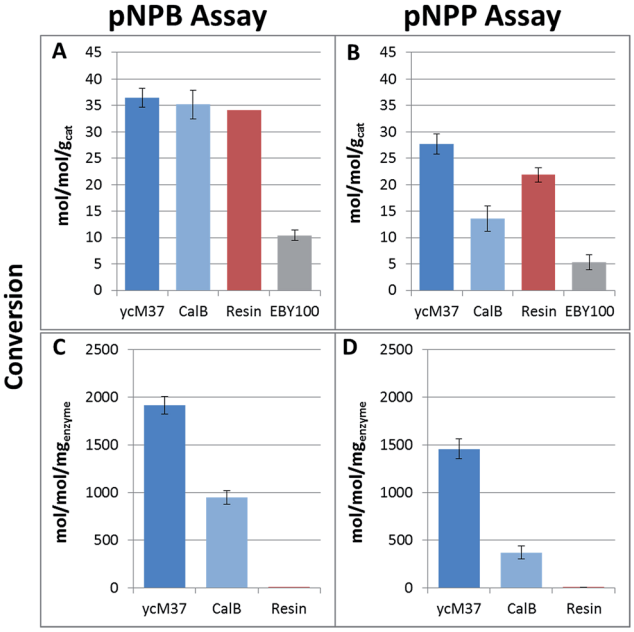


Fig. 4 Assay data for hydrolysis of *p*-nitrophenyl butyrate at 30 °C (A) and *p*-nitrophenyl palmitate at 45 °C (B). The activity of either YSD biocatalyst is comparable to that of the standard on a mass basis. When assay data are normalized by estimated protein loading (C and D), the specific activities of the YSD biocatalysts are much higher than that of the resin. Values are average of three samples; error bars are standard deviations for the same samples. The values for ycM37L and CalB represent the respective lipases immobilized *via* YSD. EBY100 is untransformed, induced yeast.

### Hydrolysis activity assays

The yeast biocatalyst successfully produces the indicator (*p*-nitrophenol) from both small (butyrate, pNPB) and large (palmitate, pNPP) nitrophenol esters (Scheme 1), as demonstrated in Fig. 4. When used at the same mass loading as a commercial lipase immobilized on a macroporous resin, the performance of the YSD biocatalyst is comparable to or better than the commercial catalyst under the conditions studied. The conversion with lipase-displaying yeast cells is significantly higher than untransformed cells and is higher than that of cells expressing a non-catalytic protein in the construct (EGFP, ESI†).

The temperature dependence of the yeast biocatalyst's performance is similar to lipase immobilized on other supports. Cells displaying CalB have an optimum temperature around 40 °C, which aligns with literature reports of a $T_{opt}$ for the enzyme between 40 and 50 °C.[19] Cells displaying ycM37L have a similar temperature profile, conflicting with reports in the literature of a $T_{opt}$ near 25 °C for free enzyme,[29] which suggests that immobilization has a stabilizing effect.[1] The lower activity at 30° is due to a twofold increase in micelle diameter (from 20 to 30 degrees), which results in a much lower accessible surface area for the reaction. This was confirmed by dynamic light scattering experiments with the assay emulsion (ESI†). At 40 °C and higher, the emulsion is unordered, rendering micelle size irrelevant. Adding iso-propanol to the assay at 5% by volume stabilizes the micelles, and a steady increase in activity is observed between 20 and 30 degrees (Fig. 5B). Above 40 °C, with and without iso-propanol, a combination of heat and detergent begin to disrupt the yeast cell and denature the enzyme. This effect leads to the steady rise in activity from the untransformed cells, as well as the decrease in activity from both the experimental and control samples (Fig. 5A). For this reason, pNPB assays were run at lower temperatures, while the solubility of *p*-NPP dictated a higher temperature.

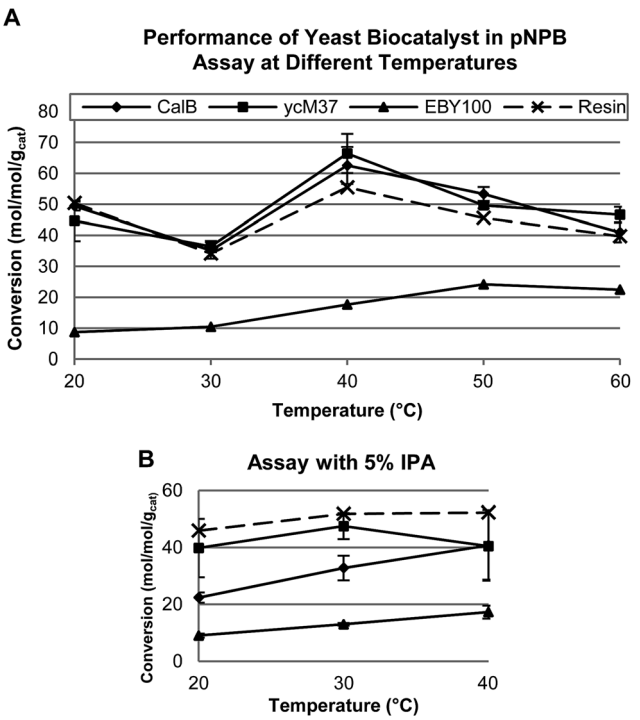


Fig. 5 Hydrolysis of *p*-nitrophenyl butyrate at different temperatures. A: without alcohol added. B: assay with 5% v/v iso-propanol added. CalB: diamonds, ycM37L: triangles, untransformed EBY100: squares, macroporous resin-immobilized lipase: circles.

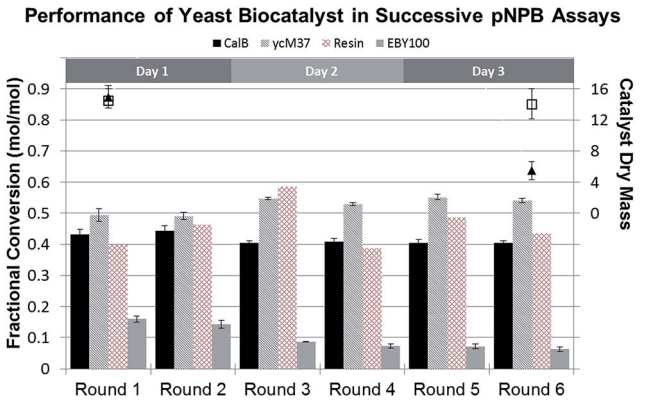


Fig. 6 Use of yeast biocatalyst in multiple assays at 30 °C. Cells and resin were washed twice with 1 mL potassium phosphate buffer between rounds. Pelleted cells and resin were stored at 4 °C overnight after rounds 2 and 4. Conversion (bars) is the average of three experiments. The dry masses of the resin and YSD catalysts (squares and triangles, respectively) were measured before and after the experiment.

The yeast biocatalyst can be re-used in the pNPB assay. Cells were washed with potassium phosphate buffer between assays and recovered by centrifugation. While loss of the biocatalyst mass was observed in the wash and recovery steps, little decrease in conversion over multiple runs was observed (Fig. 6). The conversion is shown normalized by catalyst loading in Fig. 7.

### Esterification activity assays

Esterification reactions are of greater commercial importance; once the hydrolysis performance of the two YSD systems was

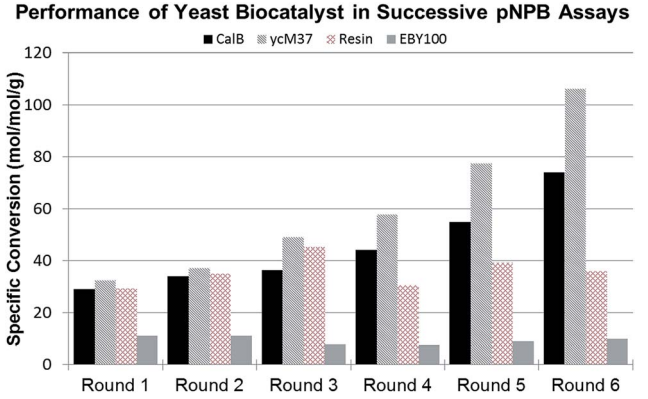


Fig. 7 Use of yeast biocatalyst in multiple assays at 30 °C. Conversions (Fig. 7) were normalized with estimated catalyst dry mass.

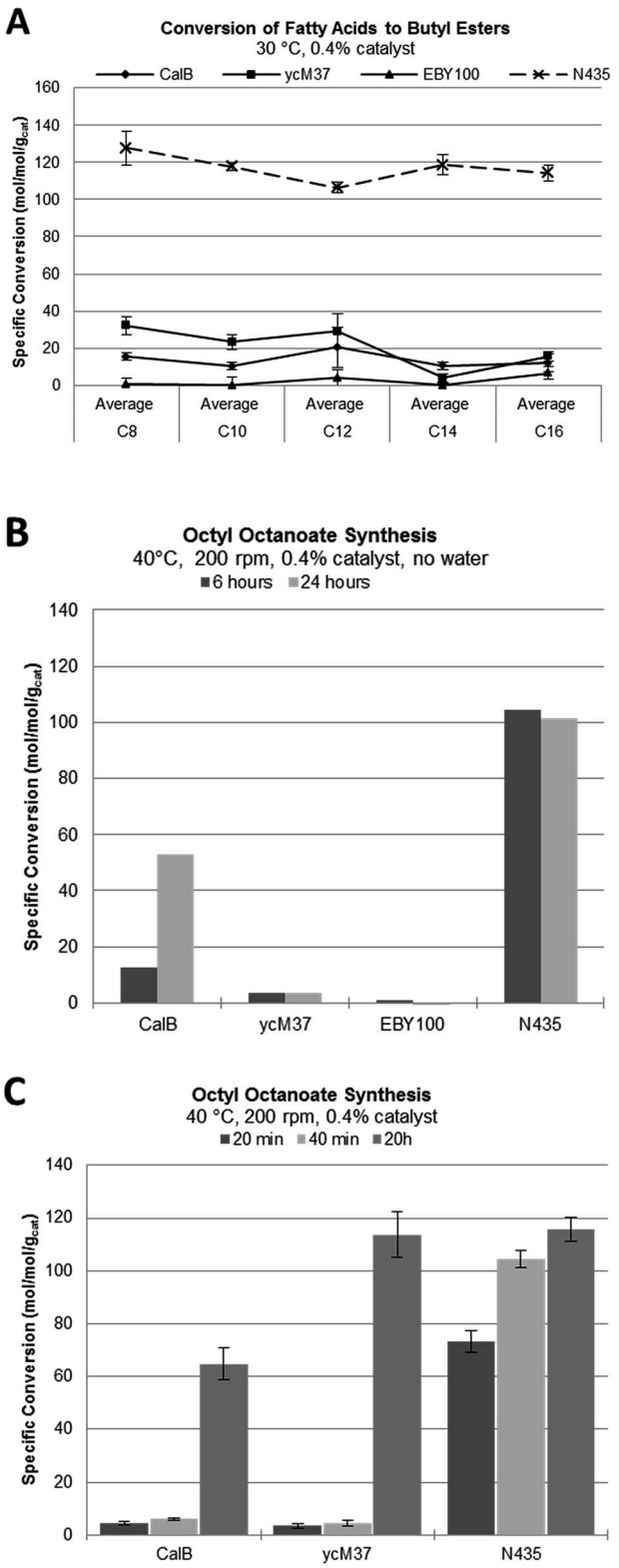


Fig. 8 The YSD biocatalyst synthesized esters of saturated fatty acids and butanol (A) or octanol (B and C). Dry catalyst was added to reaction vials. A solution of alcohol and fatty acid (both 100 mM in heptane) was added. Water (0.5% v/v [A] or 0.4% v/v [C]) was slowly added. Samples were taken after six hours (A) or as indicated (B and C). Data with error bars are averages of at least three trials, and standard deviations are shown as error bars.

benchmarked relative to Novozym 435 (N435), an esterification reaction was investigated to establish the relevance of the YSD approach. Under the conditions studied, both YSD CalB and ycM37L produced the butyl or octyl esters. Conversion of *n*-butanol and fatty acids of varying length to their respective esters is presented in Fig. 8A. The YSD biocatalysts displaying CalB and ycM37L exhibited similar preference for acyl donor chain length, with the highest conversion to the butyl ester from the shortest fatty acid (octanoic acid, C8). Further tests of the catalysts' efficacy with a water-insoluble alcohol (1-octanol) also yielded an octanoate ester (Fig. 8B). In contrast to the hydrolysis reactions, the untransformed control did not consume any fatty acid. The commercial resin apparently reached equilibrium within six hours regardless of substrate; that is, no further fatty acid was consumed. Based on the extent of the octyl octanoate reaction before equilibrium, the turnover rate for N435 is 15–20 times that of the YSD biocatalyst.

## Discussion

### Flow cytometry

Under the culture conditions routinely used to produce the biocatalyst, the majority (>60%) of cells carrying the single-copy vectors are carrying the SD construct. Sub-optimal lyophilization conditions (inadequate vacuum, solids loading too high or too low, or temperature too high), reduce the SD-carrying population fraction by approximately 10%. However, reductions of the same magnitude are observed after storage of the live cells at 4 °C after only three days, suggesting that lyophilization leads to better long-term stability. A similar decrease is observed in the number of cells that fall into the "normal, healthy" gate (P2 in Fig. 1). It is assumed that the reduction is due to cell lysis or physical deformation, and that the impact is the same for lipase-displaying and non-displaying cells. Optimized lyophilization reduces the SD-carrying population fraction less than 5% (ESI†). However, all lyophilized cells are permeable to propidium iodide, which suggests partial disruption of the cell membrane and cell wall. Lyophilization's impact on the activity of the biocatalyst as a bulk material is not clear, but it is assumed that less damage to the cells corresponds to less damage to the surface-displayed protein. Lyophilization with a cryoprotectant may improve cell integrity, but additives would likely complicate downstream applications.

The observed copy number agrees with previously reported values for the Aga2-based SD system ($5 \times 10^5$).[28] The amount of enzyme in the bulk YSD biocatalyst was calculated, based on the factors given in Table 2. Molecular weights for the enzymes were calculated from their putative amino acid sequences. The number of cells per gram of dry weight (g dw) was taken from vendor estimates for brewers' yeast. The expressing population fractions were taken from Fig. 2, and those fractions are assumed to display the average number of enzymes. The copy number and protein loading of the YSD ycM37L biocatalyst was approximately half that of YSD CalB.

 

Table 2 Estimated enzyme loading in YSD biocatalyst. Calculation of protein in the biocatalyst (in mg of protein per gram dry weight of biocatalyst) is based on flow cytometry data for copy number and fraction of the population expressing the construct

| | Molecular weight (Da) | Enzymes per cell | Number of cells expressing | Cells per g dw | mg protein per g dw biocatalyst |
|---|---|---|---|---|---|
| CalB | 33 030 | 48 422 | 70% | $2.00 \times 10^{10}$ | 0.037 |
| ycM37L | 38 026 | 22 739 | 65% | $2.00 \times 10^{10}$ | 0.019 |

### SD expression

The multi-copy vectors, under the control of a strong promoter, appear to have over-burdened the cells' synthesis and secretion pathways (Fig. 3). Weaker promoters or smaller fusion constructs may improve expression; however, others reported success with a YSD biocatalyst using Flo1S in a high-copy vector under the control of an isocitrate lyase promoter,[7] a promoter of comparable strength to Gal7.[30] With no quantitative surface coverage or population data, comparisons with these results are without merit.

### Activity assays

The YSD biocatalyst performs as well as commercial lipase immobilized on a macroporous resin in the assays under the conditions tested. The activity of CalB and ycM37L are comparable, as previously reported for free enzyme.[15] The activity has been normalized with the mass of the catalyst so that comparisons with other lipase-based catalysts may be made on an equal basis (catalyst mass loading). Since the protein is immobilized on an insoluble particle, recovery of the catalyst is a matter of simple centrifugation or filtration, both of which are routinely scaled to industrial applications. The catalyst's reusability was demonstrated here. The robustness of the yeast cell as a support is underpinned by the durability of the polysaccharide and mannoprotein cell wall, which is tolerant to solvents as well as relevant temperature and pH ranges. However, there will be some threshold where the cell support begins to break down, where the activity of the control cells approaches that of the lipase-displaying cells. Presumably, the cells are lysing and releasing endogenous hydrolases and other lytic proteins into the local environment. Judging by the performance of the untransformed cells here, that threshold is above the upper limit of the proteins' thermal stability, and will not significantly affect the performance of the yeast biocatalyst in most applications.

The resin (N435) produces esters of butanol and octanol more quickly, irrespective of the fatty acid or alcohol chain length. No acyl donor size preference is discernible for N435 because the reactions reach equilibrium before the six-hour sampling time. The addition of water to the reaction hydrates the enzyme, but also causes aggregation of the cells. The additional water is necessary for ycM37L to function in an organic environment, but not for CalB.[31] The necessity of water for ycM37L activity is apparent in Fig. 8C when compared to Fig. 8B. Water also benefits CalB to a lesser extent, as a slight improvement is observed between both the YSD CalB- and N435-catalyzed reactions (Fig. 8B and C). The octyl octanoate reaction reaches equilibrium within 2 hours if catalysed by N435, while the YSD biocatalysts need 24–48 hours (data for longer experiments not shown). The reaction is significantly impeded if cells aggregate to an extent that their uniform suspension in the reaction suffers (see CalB results in Fig. 8B, which suffered from catalyst clumping). The disparity between the esterification activity of the YSD biocatalysts and N435 is

Table 3 Cost estimates for production of the YSD biocatalyst

| | Current (lab-scale) production | | | Theoretical production | |
|---|---|---|---|---|---|
| | Nutrient requirement | Current price | Bulk cost[a] | Bulk cost[e] | Nutrient source |
| Galactose | 40 g/batch | %15 per kg | %50 | %8.33 | Beet sugar, %2.50 per kg |
| Ammonium sulfate | 10 g/batch | %50 per kg | %42 | | |
| Nitrogen/vitamin base | 3.4 g/batch | %1 per g | %283 | %1.61 | Fish meal, %0.8 per kg |
| Amino acids | 4 g/batch | %310 per kg | %103 | | |
| Water (sterile + disposal) | 4 L/batch | <%2 per MT | %0.19 | %0.19 | |
| **Media** | | | **%478** | | |
| Lyophilization[b] | | | %108 | %108 | |
| Coolant, −50 °C | [c] | %13.11 per GJ | %4.60 | | |
| Plant air | 140 L chamber | %0.35 per std $m^3$ | ≈0 | | |
| Electricity (3/4 hp vacuum) | 70% efficiency | %0.06 per kWh | %3.45 | | |
| Maintenance | [d] | %10 000 per year | %100 | | |
| **Total** | **%586** | | | **%118** | |

[a] Assumes yield of 30 g dry cells per 100 g of galactose, scaled up for 1 kg dry cells. [b] Assumes single 3 day cycle for 1 kg of dry cells, dried to 5% moisture. [c] Assumed cell slurry is 5% solids, removed 95% of moisture. [d] Assumed 300 working days per year. [e] Bulk prices quoted from vendors for 100 kg, current as of April 2014.

intriguing, particularly in light of the comparable performance in hydrolysis assays. This is a particularly interesting result because the YSD CalB and N435 are both CalB-centric systems. Comparable esterification data for ycM37L could not be found in the literature. It is unclear whether the difference is one of specific protein modifications introduced to N435, the relative protein loadings, or the surface chemistry of the acrylic bead *versus* the yeast cell.

There are significant differences between the resin and the yeast cell in terms of surface environment and protein concentration. The difference in surface polarity may play a greater role in the hydrophobic ester synthesis reactions than it does in a surfactant-mediated hydrolysis assay. Previous attempts to demonstrate a YSD biocatalyst in ester synthesis have used more polar reactants.[26,32–34] Heptane ($\log P = 4.3$), unsaturated fatty acids ($\log P$ from 3.1 for octanoic acid to 7.2 for hexadecanoic acid), and 1-octanol are highly hydrophobic. While butanol is more polar ($\log P = 0.84$), it is not miscible with water. The local concentration of the hydrophobic substrates near the cell surface—which likely collects any available water—could be lower than that near the surface of the hydrophobic resin. A locally water-rich environment on the cell surface could create a transport barrier between the enzyme and the bulk solvent. Despite the difference in apparent esterification activity, the performance on a bulk mass basis reflects a significant improvement in terms of cost.

### Cost comparison

Since the YSD biocatalyst is as active (hydrolytically) as commercialized formulations of immobilized lipase, the production cost can be compared to the commercial purchase price to inform the sourcing decision. A plasmid-based production strain is unlikely since chromosomal integration is typical, so the strains used in this work provide a useful base-case. Excluding the costs associated with cloning and screening, the estimated cost of production from seed culture to lyophilized final product are indicated in Table 3. This analysis assumes that galactose is the limiting nutrient; the bulk price for the grade used in these studies is %15–%30 per kg, which was used in the cost analysis. The costs of the other media components are assumed equal to or less than the largest lab-scale quantities available. The energy and projected maintenance costs for lyophilization are included, based on the equipment used in this study. Additional costs for waste treatment and peripheral utilities (plant air and DI water) are also included. Assuming a carbon efficiency of 30% (kg dry cells per kg galactose), the cost of one kilogram of the YSD biocatalyst is %590 to %640 for the galactose prices mentioned previously. The theoretical production reflects potential cost savings from complex nutrient sources. Compared to %11 250 per kg, the bulk price for the lipase resin used in this study, the YSD biocatalyst represents significant cost savings without changing the catalyst loading or batch productivity—irrespective of the application. Comparisons with other commercial lipase sources (Table 4) are less favorable, but the conservative theoretical production cost of the YSD biocatalyst is still less than that of other readily available commercial lipases.

Because the apparent activity of the YSD biocatalysts changes in different applications, the predicted cost of manufacture was normalized with the measured activity in order to provide a rational basis for comparison. In an aqueous environment (geared towards hydrolysis), the calculus based on mass loading does not differ meaningfully. However, in non-polar environments geared toward organic synthesis, the order-of-magnitude difference in conversion rate puts the YSD biocatalyst behind N435 by a factor of nearly two.

The estimated protein loading in N435 is 30 mg per g $dw^{-1}$.[35] This figure puts the amount of protein in the commercial system at roughly three orders of magnitude more than the YSD system. Given this inequality, an order of magnitude difference in rate is unsurprising. Cost comparison on a per-enzyme basis will not favor the YSD system, nor will comparisons in synthetic applications. However, the relative activity on a per-enzyme basis (Fig. 4C and D) suggests that the YSD system is a far more efficient scaffold for lipase production. This holds true in non-polar environments, where N435 is only an order of magnitude faster, despite presenting three orders of magnitude more enzyme.

## Experimental

### Strains and media

Plasmid DNA was screened and stored in *Escherichia coli* DH5α. The untransformed strain was cultivated in LB media (10 g $L^{-1}$ tryptone, 5 g $L^{-1}$ yeast extract, 5 g $L^{-1}$ sodium chloride, 1 mL 1 N sodium hydroxide) at 37 °C and made electrocompetent in-house and transformed as described in *Molecular Cloning*.[36] After electroporation, cells were recovered in SOC media

Table 4 Cost comparison for the YSD biocatalyst and commercial lipase sources

| | Price per kg | Price per kg-U[e] (hydrolysis, pNPB) | Price per kg-U[e] (hydrolysis, pNPP) | Price per kg-U[e] (synthesis) |
|---|---|---|---|---|
| YSD biocatalyst (lab-scale)[a] | %586 | %16 | %28 | %151 |
| YSD biocatalyst (theoretical)[a] | %118 | %3 | %6 | %30 |
| Novozym 435 (bulk, from Sigma Aldrich)[b] | %11 250 | %330 | %516 | %153 |
| Novozym 435 (bulk, commercial)[c] | %1200 | %35 | %55 | %16 |
| TransBiodiesel[d] | %150–300 | Not tested | Not tested | Not tested |

[a] Current work. [b] Quote from Sigma-Aldrich, Feb. 2014. [c] Glycerin Carbonate Market Research and Analysis, Piedmont Biofuels, 2010. [d] http://www.transbiodiesel.com/faq1, accessed March 9, 2014. [e] Normalized price (per kg) by average of YSD biocatalyst activities in Fig. 4 and 20 min time point in Fig. 8B.

 

(20 g $L^{-1}$ tryptone, 5 g $L^{-1}$ yeast extract, 10 mM magnesium sulfate, 0.5 g $L^{-1}$ sodium chloride, 250 mM potassium chloride, 10 mM magnesium chloride, 20 mM glucose, 1 mL 1 N sodium hydroxide) and plated with appropriate antibiotics (LB with 15 g $L^{-1}$ agar and 50 mg $L^{-1}$ ampicillin). Cultures for plasmid preparation were grown on or in LB, with antibiotics. *Saccharomyces* strain EBY100 (ref. 4) was propagated in 2× YAPD (20 g $L^{-1}$ yeast extract, 100 mg $L^{-1}$ adenine hemisulfate, 40 g $L^{-1}$ peptone, 40 g $L^{-1}$ glucose).[37] Two strains of *Saccharomyces cerevisiae*, S288C (MATα sta1 sta2 sta3 STA10) and MT8-1 (MATa ade his3 leu2 trp1 ura3), were purchased from the American Type Culture Collection (ATCC) and propagated in/on YAPD at 30 °C. Yeasts were made electrocompetent in-house,[38] with modified wash and recovery buffers.[39] After electroporation, cells were recovered in 1 : 1 2× YAPD : 1 M sorbitol and plated on minimal media or used to inoculate liquid media. Selection is maintained through the strain's tryptophan (EBY100) or uracil (MT8-1) auxotrophy. Yeasts are grown in selective (*i.e.*, lacking tryptophan/uracil) synthetic complete (SC[35]) media with 2% glucose for a carbon source and penicillin-streptomycin (100 U $mL^{-1}$ and 100 μg $mL^{-1}$, respectively) through two passes at 30 °C before being transferred to selective SC media with 2% galactose as a carbon source for induction at 20 °C.

### Cloning and transformation

All T4 ligase, phosphatase, and polymerase were obtained from New England Biolabs, Ipswich, MA. The bacterial protein sequence for M37L (NCBI accession # AAS78630) was optimized for expression in yeast by GENEWIZ (Research Triangle Park, NC) and provided in a bacterial stock containing the plasmid pUC57-ycM37L. DNA for the CalB mature peptide was provided in pET22-mCalB in bacterial stocks. Genomic DNA from *S. c.* S288C was purified using a modified protocol for a blood and tissue kit (QIAGEN, Valencia, CA).[40] The gene for FLO1S was amplified from genomic DNA using high-fidelity Phusion polymerase and previously reported primers.[7] The PCR (polymerase chain reaction) product was digested with BamHI/XhoI and ligated into BamHI/XhoI-digested pYES with T4 ligase. The construct was transformed into *E. coli* for storage. The insert was confirmed by restriction digest and sequencing. The flo1S gene was purified from an agarose gel after digesting the plasmid with BamHI/XhoI, using a spin kit (Thermo Fisher Scientific, Pittsburgh, PA). Plasmid DNA was purified from bacterial cultures with a spin kit. The lipase sequences were amplified from their plasmid templates with high-fidelity PCR.

Plasmid backbones (pCT-EGFP[41] and p426 GALL, ATCC 87341) were purified from bacterial stocks, digested with BamHI/NheI (pCT plasmids) or BamHI/EcoRI (p426 plasmids), and treated with phosphatase. For pCT-based plasmids, the PCR products of the lipases were digested with BamHI/NheI, combined individually with the plasmid backbones in 3 : 1 ratios, and ligated with T4 ligase. For p426-based plasmids, the PCR products of the lipases were digested with XhoI/EcoRI and combined with gel-purified flo1S (BamHI/XhoI) and the digested plasmid backbone in 3 : 3 : 1 molar ratios (lipase : flo1S : p426). The components were ligated with T4 ligase overnight at 16 °C. Ligation products were transformed into *E. coli* by electroporation. Putative transformants were screened for the insert by PCR (OneTaq Quick-Load Master Mix, New England Biolabs, Ipswich, MA). After the insert was detected using PCR, the identified colonies were picked for plasmid purification, restriction digest screening, and sequencing. The c-myc epitope was added to flo1S-lipase fusions and the p426 GALL backbone *via* PCR. The insert and backbone were recombined with one-step ISO assembly,[42] transformed into *E. coli*, and screened as before.

### Production of the yeast surface-display biocatalyst

Yeasts carrying the putative construct for the lipase-alpha-agglutinin fusion protein under GAL promoter control (Fig. 9) were propagated in SC/Dex (SC with 2% glucose) without tryptophan. Yeasts carrying the putative construct for the Flo1S-lipase fusion under GALL control were propagated in SC/Dex without uracil. Batches were passaged by inoculating 3 mL cultures 1 : 500 with cell slurry from previous generations and grown at 30 °C, 250 rpm in a 15 mL Falcon tube to an $OD_{600}$ of 2–3. A 200 mL culture was inoculated 1 : 200 from this culture and grown under the same conditions in baffled shaker flasks to a final $OD_{600}$ of 6–8 ($5 \times 10^7$ cells per mL). Media was removed by centrifugation (3000 g for 15 min at 4 °C) and the cell pellet was re-suspended in induction media. The suspension was used to inoculate a 2 L bioreactor (Sartorius AG, Goettingen,

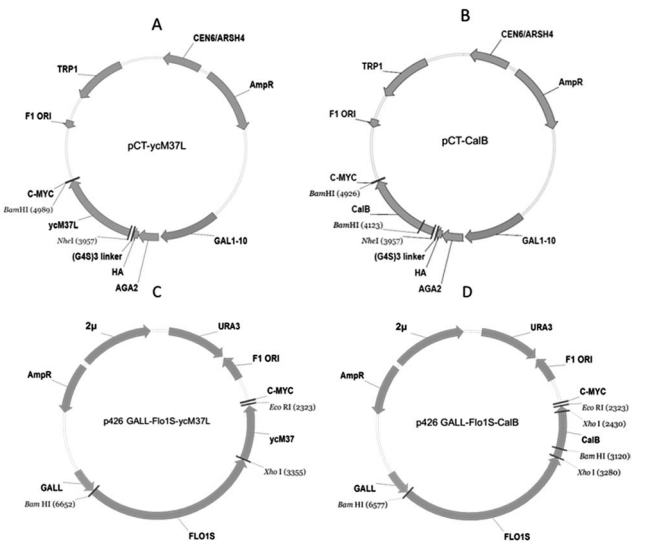


Fig. 9 Vector maps for the plasmids used in this study. A and B: YSD vectors containing ycM37L and CalB, respectively; includes bacterial origin and ampicillin resistance marker for propagation in *E. coli*, single-copy yeast replication origin (CEN6/ARSH4) and selection marker (TRP10). Transcription is induced by the GAL promoter. Secretion and surface attachment are accomplished *via* the fusion to Aga2. Immuno-labeling detects the C-terminal c-myc epitope tag. C and D: YSD vectors containing ycM37L and CalB, respectively; includes bacterial origin and selection marker, multi-copy yeast replication origin (2μ) and selection marker (URA3). Transcription is induced by the GAL promoter. Secretion and surface attachment are accomplished *via* the fusion to Flo1S. Immuno-labeling detects the C-terminal c-myc epitope tag.

Germany) and operated at 20 °C, 250 rpm with 4 L $min^{-1}$ sparged air during induction. Samples were removed at regular intervals (4–6 hours), and the sample volume (typically 10 mL) was replaced with galactose (20% weight/volume in DI water, sterilized by filtration). Induction ended after 18–20 hours, with a final cell count of 1–3 × $10^7$ cells per mL.

Following induction, the bioreactor was chilled to 6 °C and the culture siphoned into chilled centrifuge bottles. Cells were harvested by centrifugation (4000 g for 30 min at 4 °C) and washed once with 1 L sterile, cold water. Cells were re-suspended in a dense slurry in DI water (3–5 × $10^9$ cells per mL), distributed into 2 mL microcentrifuge tubes, frozen, lyophilized in a SpeedVac (Thermo SPD-111V) for >8 hours, and stored at 4 °C.

### Assays for esterase (hydrolytic) activity

Lipase from *C. antarctica* immobilized on acrylic resin was purchased from Sigma Aldrich (St. Louis, MO) and used as a positive control. Lyophilized YSD biocatalyst or resin was weighed into clean 2 mL microcentrifuge tubes. Two substrates were used for the assays: *p*-nitrophenyl butyrate (pNPB) and *p*-nitrophenyl palmitate (pNPP) (Sigma Aldrich, St. Louis, MO). An emulsion of substrate (1–4 mM in 50 mM potassium phosphate buffer, pH 6.5, with 0.5% Triton-X 100) was added to a final catalyst loading of 20 mg dw $mL^{-1}$. Iso-propanol was added to *p*-nitrophenyl palmitate assays at 5% by volume. Samples were gently agitated in a temperature-controlled water bath during the assay. The bath was maintained at 30 °C for assays using pNPB and at 45 °C for assays using pNPP (see Scheme 1), unless otherwise indicated. Aliquots of at least 20 μL were removed periodically and spun down at >10 000 g for >1 minute and the absorbance of the supernatant at 400 nm was measured on a NanoDrop 1000 (Thermo Scientific, Wilmington, DE). The maximum observed absorbance within 10 minutes was recorded, since the acrylic resin was observed to absorb some of the hydrolysis product at higher conversions, leading to under-reporting of the activity of the resin-immobilized lipase. The concentration of *p*-nitrophenol was calculated based on the absorbance and standard curves prepared in appropriate buffer.

### Esterification activity

Chemicals were GC grade or better. Dry catalyst was weighed into clean 1.5 dram glass vials. Solutions of a fatty acid and either *n*-butanol or *n*-octanol (1 mL of each, both 200 mM in heptane) were added to the vials. Palmitic acid solutions were warmed to 30 °C to dissolve the fatty acid. For the fatty acid specificity trials, water was added to the reaction at 0.5% vol/vol. The vials were sealed and moved to a magnetically stirred heat block with digital temperature control. The reactions were stirred at 200 rpm for six hours, beginning when the reaction was first heated. Samples of 50 μL were added to 1 mL of heptane and analyzed by GC-FID. The samples were analyzed on a Shimadzu GC2010 equipped with an autosampler and a DB-5 capillary column (30 m × 0.25 μm × 0.25 μm). One μL of each sample was injected at a 30 : 1 split ratio with helium as the carrier gas. The injector and detector were held at 300 °C. The oven temperature was held at 90 °C for 2 minutes, ramped to 160 °C at 20° $min^{-1}$, to 250 °C at 5° $min^{-1}$, and to 300 °C at 25° $min^{-1}$. The concentration of the fatty acid was determined by comparing the FID peak area to standard curves prepared in heptane.

### Flow cytometry

Yeast cells (8 × $10^6$ to 5 × $10^7$) were suspended in 1 mL phosphate buffered saline supplemented with bovine serum albumin (PBS–BSA, 137 mM sodium chloride, 2.7 mM potassium chloride, 10 mM dibasic sodium phosphate, 2 mM monobasic potassium phosphate, 1 g $L^{-1}$ BSA in water). The suspension was centrifuged at 10 000 g for 30 s (subsequent centrifugations used the same conditions) and re-suspended in 250 μL PBS–BSA. Primary antibody (chicken anti-c-myc, Invitrogen) was added at a 1 : 250 dilution and mixed by vortexing. After >15 minutes at room temperature, the cells were diluted with 1 mL PBS–BSA, centrifuged, and the supernatant was aspirated. The cells were washed with 1 mL PBS–BSA, centrifuged, and aspirated again. Secondary antibody (goat anti-chicken Alexa 633, Invitrogen) was added at a 1 : 250 dilution in 250 μL PBS–BSA. After >15 minutes at room temperature in the dark, the cells were diluted and washed with PBS–BSA in the same way. Cells were re-suspended in 1 mL PBS–BSA and vortexed immediately before data collection. Data were collected on an Accuri C6 cytometer with at least 30 000 events per run and slow fluidics. The manufacturer's software was used for analysis. Normal, healthy cells were gated in the FSvSS plots based on an unlyophilized, untreated, untransformed control (Fig. 1). This gate was applied to histograms of Alexa 633 fluorescence (Fig. 2 and 3), which were used to determine the fraction of the population expressing the surface display (SD) construct. The baseline for expression was determined by experimental samples incubated without the primary antibody (Fig. 2).

Copy number was determined by comparing labeled cells to a standard curve drawn through four groups of antibody coated beads with known antibody binding capacities (Simply Cellular anti-Mouse IgG, Bangs Labs, Fishers, IN). Lyophilized cells (2 × $10^6$) and the anti-mouse IgG microspheres were suspended in PBS–BSA. Fluorescein-conjugated mouse anti-c-cymc antibody (Sigma) was added, 10 μg to 200 μL of cell suspension or to 100 μL of bead suspension. After incubating for 30 minutes at room temperature and protected from light, the beads and cells were washed twice with PBS–BSA and re-suspended in 500 μL for analysis on an Accuri C6 cytometer. According to the manufacturer's instructions, half-height, full-width gates were drawn on the standards and labeled cell populations. The mean fluorescence intensity of the gated standards was used to draw the standard curve from which the copy number of the labeled cells was interpolated.

## Conclusions

In terms of hydrolytic activity, the YSD catalyst is comparable to commercial immobilized lipase catalysts at equal mass loadings, but not as effective in non-aqueous applications. The biocatalyst can be re-used in the same manner as a bead-based catalyst, with the additional benefit of a greater surface-to-

 

volume ratio, but at a size that can easily be removed from suspension by centrifugation or routine filtration. The yeast cell appears to confer significant thermal stability upon ycM37L, and the thermal stability of YSD CalB was similar to that of a commercial acrylic bead-based system. Lipase produced with YSD is more efficient on a per-enzyme basis than lipase in N435.

## Acknowledgements

The authors gratefully acknowledge Sonia Herrero from Professor Margo Daub's lab at NCSU for donating a lab strain of *E. coli*; Professor Balaji Rao's lab for donating the pCT-EGFP vector, the stocks for EBY100, and time on the cell sorter; and Kerri Cushing for donating the pET22-CalB vector. This work (JE) was supported in part by NSF award 0832498 through the Center for BioEnergy Research and Development, by the GAANN Interdisciplinary Doctoral Program in Molecular Biotechnology, award P200A090129-11, and by the Eastman Chemical Center of Excellence. The authors declare no conflicts of interest.

## Notes and references

1 C. Mateo, J. M. Palomo, G. Fernandez-Lorente, J. M. Guisan and R. Fernandez-Lafuente, *Enzyme Microb. Technol.*, 2007, **40**, 1451–1463.
2 A. Illanes, *Enzyme biocatalysis: principles and applications*, Springer, New York, 2008.
3 P. Tufvesson, J. Lima-Ramos, M. Nordblad and J. M. Woodley, *Org. Process Res. Dev.*, 2010, **15**, 266–274.
4 E. T. Boder and K. D. Wittrup, *Nat. Biotechnol.*, 1997, **15**, 553–557.
5 M. Ueda and A. Tanaka, *J. Biosci. Bioeng.*, 2000, **90**, 125–136.
6 C. E. Ballou, *Cold Spring Harbor Monograph Archive*, 1982, vol. 11, pp. 335–360.
7 T. Matsumoto, H. Fukuda, M. Ueda, A. Tanaka and A. Kondo, *Appl. Environ. Microbiol.*, 2002, **68**, 4517–4522.
8 N. Gera, M. Hussain, R. C. Wright and B. M. Rao, *J. Mol. Biol.*, 2011, **409**, 601–616.
9 Y. Fujita, S. Takahashi, M. Ueda, A. Tanaka, H. Okada, Y. Morikawa, T. Kawaguchi, M. Arai, H. Fukuda and A. Kondo, *Appl. Environ. Microbiol.*, 2002, **68**, 5136–5141.
10 P. Villeneuve, J. M. Muderhwa, J. Graille and M. J. Haas, *J. Mol. Catal. B: Enzym.*, 2000, **9**, 113–148.
11 A. M. Klibanov, *Trends Biochem. Sci.*, 1989, **14**, 141–144.
12 J. Uppenberg, N. Oehrner, M. Norin, K. Hult, G. J. Kleywegt, S. Patkar, V. Waagen, T. Anthonsen and T. A. Jones, *Biochemistry*, 1995, **34**, 16838–16851.
13 Y. Shimada, Y. Watanabe, T. Samukawa, A. Sugihara, H. Noda, H. Fukuda and Y. Tominaga, *J. Am. Oil Chem. Soc.*, 1999, **76**, 789–793.
14 J. H. Yoon, *Int. J. Syst. Evol. Microbiol.*, 2005, **55**, 335–339.
15 K. S. Yang, J. Sohn and H. K. Kim, *J. Biosci. Bioeng.*, 2009, **107**, 599–604.
16 T. P. Korman, B. Sahachartsiri, D. M. Charbonneau, G. L. Huang, M. Beauregard and J. U. Bowie, *Biotechnol. Biofuels*, 2013, **6**, DOI: 10.1186/1754-6834-6-70.
17 S. H. Lee, J. Choi, M. Han, J. H. Choi and S. Y. Lee, *Biotechnol. Bioeng.*, 2005, **90**, 223–230.
18 S. Tamalampudi, S. Hama, T. Tanino, M. R. Talukder, A. Kondo and H. Fukuda, *J. Mol. Catal. B: Enzym.*, 2007, **48**, 33–37.
19 M. Kato, J. Fuchimoto, T. Tanino, A. Kondo, H. Fukuda and M. Ueda, *Appl. Microbiol. Biotechnol.*, 2007, **75**, 549–555.
20 S. Shiraga, M. Kawakami, M. Ishiguro and M. Ueda, *Appl. Environ. Microbiol.*, 2005, **71**, 4335–4338.
21 G. Su, X. Zhang and Y. Lin, *Biotechnol. Lett.*, 2010, **32**, 1131–1136.
22 A. Bielen, R. Teparic, D. Vujaklija and V. Mrsa, *Food Technol. Biotechnol.*, 2014, **2014**, 16–34.
23 W. Zhang, S. Han, D. Wei, Y. Lin and X. Wang, *J. Chem. Technol. Biotechnol.*, 2008, **83**, 329–335.
24 A. Yoshida, S. Hama, K. Nakashima and A. Kondo, *Enzyme Microb. Technol.*, 2011, **48**, 334–338.
25 T. Tanino, T. Aoki, W. Chung, Y. Watanabe, C. Ogino, H. Fukuda and A. Kondo, *Appl. Microbiol. Biotechnol.*, 2009, **82**, 59–66.
26 S. Han, Z. Pan, D. Huang, M. Ueda, X. Wang and Y. Lin, *J. Mol. Catal. B: Enzym.*, 2009, **59**, 168–172.
27 J. Han and H. Kim, *J. Microbiol. Biotechnol.*, 2011, **21**, 1159–1165.
28 S. Shibasaki, M. Ueda, T. Iizuka, M. Hirayama, Y. Ikeda, N. Kamasawa, M. Osumi and A. Tanaka, *Appl. Environ. Microbiol.*, 2001, **55**, 471–475.
29 H. S. Ryu, H. K. Kim, W. C. Choi, M. H. Kim, S. Y. Park, N. S. Han, T. K. Oh and J. K. Lee, *Appl. Microbiol. Biotechnol.*, 2005, **70**, 321–326.
30 K. Umemura, H. Atomi, T. Kanai, Y. Teranishi, M. Ueda and A. Tanaka, *Appl. Microbiol. Biotechnol.*, 1995, **43**, 489–492.
31 J. Eby and S. W. Peretti, *RSC Adv.*, submitted
32 Z. Pan, Z. Yang, L. Pan, S. Zheng, S. Han and Y. Lin, *J. Ind. Microbiol. Biotechnol.*, 2014, **41**, 711–720.
33 Z. Jin, J. Ntwali, S. Han, S. Zheng and Y. Lin, *J. Biotechnol.*, 2012, **159**, 108–114.
34 Z. Jin, S. Liang, X. Zhang, S. Han, C. Ren, Y. Lin and S. Zheng, *Biotechnol. Bioprocess Eng.*, 2013, **18**, 365–374.
35 Z. Cabrera, G. Fernandez-Lorente, R. Fernandez-Lafuente, J. M. Palomo and J. M. Guisan, *J. Mol. Catal. B: Enzym.*, 2009, **57**, 171–176.
36 J. Sambrook, *Molecular cloning: a laboratory manual*, Cold Spring Harbor Laboratory Press, Cold Spring Harbor, N.Y., 2001.
37 D. R. Gietz and R. A. Woods, in *Methods in Enzymology*, ed. C. Guthrie and G. R. Fink, Academic Press, 2002, pp. 87–96.
38 D. M. Becker and V. Lundblad, in *Current Protocols in Molecular Biology*, John Wiley & Sons, Inc., 2001.
39 N. Gera, M. Hussain and B. M. Rao, *Methods*, 2013, **60**, 15–26.
40 C. S. Hoffman, in *Current Protocols in Molecular Biology*, John Wiley & Sons, Inc., 2001.
41 M. F. Canbolat, N. Gera, C. Tang, B. Monian, B. M. Rao, B. Pourdeyhimi and S. A. Khan, *ACS Appl. Mater. Interfaces*, 2013, **5**, 9349–9354.
42 D. G. Gibson, in *Methods in Enzymology*, Academic Press, 2011, pp. 349–361.